Monthly Notices
of the
ROYAL ASTRONOMICAL SOCIETY

MNRAS **456,** 518–524 (2016) doi:10.1093/mnras/stv2710

Kr II transition probability measurements for the UV spectral region

M. T. Belmonte,[1⋆] L. Gavanski,[2] R. J. Peláez,[3] J. A. Aparicio,[1⋆] S. Djurović[2] and S. Mar[1⋆]

[1]*Departamento de Física Teórica, Universidad de Valladolid, Atómica y Óptica, Paseo de Belén 7, E-47011 Valladolid, Spain*
[2]*Faculty of Sciences, Department of Physics, University of Novi Sad, Trg Dositeja Obradovića 4, 21000 Novi Sad, Serbia*
[3]*Laser Processing Group, Instituto de Óptica, CSIC, Serrano 121, E-28006 Madrid, Spain*

Accepted 2015 November 17. Received 2015 November 14; in original form 2015 August 30

ABSTRACT

The determination of radiative transition probabilities or oscillator strengths is of common interest in astrophysics. The analysis of the high-resolution stellar spectra is now available in order to estimate the stellar abundances. In this paper, 93 experimentally obtained transition probability values (A_{ki}) for singly ionized krypton spectral lines belonging to the ultraviolet (UV) wavelength region (208–360) nm are presented. These data, expressed in absolute units, were derived from the measurements of relative spectral line intensities and the values of transition probability data taken from the literature. The results obtained extend considerably the transition probability data base. As a light source, a plasma from a low-pressure pulsed arc was used. Its electron density was in the range of (1.5–3.4) $\times$ 10^{22} m^{-3}, while the temperature was between 28 000 and 35 000 K. A detailed analysis of the results is also given. Only a few relative and a few absolute transition probabilities from other authors, for the mentioned spectral region, are available in the literature.

Key words: line: profiles – plasmas – techniques: spectroscopic.

1 INTRODUCTION

Krypton is present in many light sources and lasers as the working gas (Shimoda 1984), it is one of the inert gases used in spectral lamp production and development (Cayless & Marsden 1983) and it also appears in fusion experiments (Loch et al. 2002). On the basis of the measurements of Planetary Nebulae spectra, it was found that krypton is one of the most abundant elements in the cosmos with $Z > 32$ (Dinerstein 2001; Sharpee et al. 2007). It has been detected in stellar atmospheres (Bidelman 1962), in the interstellar medium (Cardelli, Savage & Ebbets 1991; Cardelli & Meyer 1997), in the solar wind (Morton 2000) and recently in a white dwarf (Werner et al. 2012). Krypton is used as propellant in electric propulsion systems and Kr II spectral lines are used for the characterization of ions' velocity distribution functions by means of laser fluorescence in Hall thrusters (Mazouffre & Pawelec 2009). Transition probabilities data are of fundamental importance in the determination of plasma temperatures from the intensities of the spectral line radiation (Griem 1964). Radiative lifetimes for forbidden transitions of ultraviolet (UV) Kr II lines have been analysed recently (Träbert 2012; Saito et al. 2015), but there are not so many papers devoted to electric dipole UV Kr II transition probability measurements. The papers Marantz, Rudko & Tang (1969), Miller, Roig & Bengtson (1972), Fonseca & Campos (1982) and Djeniže, Milosavljević & Dimitrijević (2003) report relative transition probabilities, mostly for transitions in the visible part of the spectrum. Only the paper Fonseca & Campos (1982) reports relative results for several UV transitions. Transition probability results in absolute units are given in Podbiralina, Smimov & Stegnova (1973), Helbig (1978), Brandt, Helbig & Nick (1982), Bertuccelli & Di Rocco (1991), Dzierżega et al. (2001), de Castro et al. (2001), Rodríguez et al. (2001) and Mar et al. (2006) and they generally cover the wavelength region between 360 and 714 nm. Results for a wide wavelength region (200–2400 nm) have only been reported in Dzierżega et al. (2001). Some authors report data about lifetime measurements (Fonseca & Campos 1982; Schade et al. 1989; Das & Bhattacharya 1992; Jullien et al. 1993; Das 1997; Lauer et al. 1999).

We can divide the experimental transition probability data found in the bibliography for the UV region into two different groups, depending on the method used for the measurement of the A_{ki} values. Results from Helbig (1978) have been obtained by quantitative spectroscopy of a plasma source in local or partial local thermodynamic equilibrium (pLTE). As mentioned in Dzierżega et al. (2001), this method has to deal with uncertainties around 20 per cent due to the difficulties to either characterize the source or achieve thermal equilibrium conditions. Results from Podbiralina et al. (1973) and Dzierżega et al. (2001) have been obtained by normalizing measured branching ratios with upper-level lifetime data. This method has a disadvantage concerning the necessity of measuring all the possible transitions from this upper level. In this article, we compare our

⋆E-mail: teruca@opt.uva.es (MTB); juanantonio.aparicio@uva.es (JAA); santiago@opt.uva.es (SM)

new data, which have been measured by quantitative spectroscopy, with data from Dzierżega et al. (2001) obtained in a branching ratio experiment. This comparison is especially interesting because it relates data obtained by the two different methods.

In this paper, we continue with the measurements of A_{ki} values carried out in our laboratory (de Castro et al. 2001; Rodríguez et al. 2001; Mar et al. 2006) for Kr II, extending the spectral range to the UV. We report absolute transition probability data for 93 Kr II lines belonging to 69 multiplets within the 208–360 nm spectral range. These values were obtained by measuring the relative intensities of the spectral lines under study. In order to transform our relative measurements into absolute ones, we have selected seven spectral lines and taken their transition probability value from the bibliography (Mar et al. 2006; Kramida et al. 2015). The measurements were carried out by using a plasma produced in a low-pressure pulsed arc as a light source. The electron density, which was in the range of (1.5–3.4) $\times$ 10^{22} m^{-3}, was determined by using a two-wavelength interferometric method. The plasma temperature is the most important plasma parameter for the measurement of the transition probabilities. The excitation temperature, in the range of 28 000–35 000 K, was determined by using the Boltzmann-plot method for seven spectral lines whose transition probabilities were taken from the bibliography (Mar et al. 2006; Kramida et al. 2015). It should also be noted here that the plasma conditions satisfy the pLTE criterion for all the considered instants of measurement.

2 EXPERIMENT

2.1 Set-up

The spectral line intensities have been measured from a low-pressure pulsed arc plasma source. More details concerning the experimental arrangement can be found in Gigosos et al. (1994), Val et al. (1998) and Ćirišan et al. (2011). Here, only a short description will be given for completeness. The discharges were carried out through a cylindrical tube made of Pyrex glass, 175 mm long and 19 mm in internal diameter. Pure krypton at a pressure of 120 Pa was continuously flowing through the discharge tube at a rate of 0.3 sccm. Plasma pulses were created by discharging a capacitor bank of 20 μF through the discharge tube. The capacitor bank was charged up to 7.8 kV. The plasma life was about 200 μs. In order to ensure the plasma reproducibility, the gas in the tube was preionized by using a continuous current of several mA. The discharge tube has been designed to avoid sputtering as much as possible (Val et al. 1998). In spite of this fact, the windows closing the tube were replaced every 800 discharges in order to reduce the optical transmittance loss to values under 5 per cent. Furthermore, the electrodes were polished several times during the experiment.

The spectra were recorded by using a Jobin–Yvon spectrometer, 1.5 m focal length, with a UV holographic grating, 2400 lines mm^{-1}. The spectral resolution of our spectrometer has already been calibrated (Peláez et al. 2012) and it is 3 pm per channel approximately within the working spectral range of this experiment. This resolution gives an idea of the ability of our device to resolve very close spectral lines and it will be important for further discussion. The spectrometer was equipped with an intensified charge-coupled device (ICCD) as a photo-detector. The spectra were taken along the discharge tube, 2 mm off the tube axis, at the instants 50, 60, 100, 110 and 130 μs after the beginning of the discharge. The exposure time varied between 2 and 5 μs and it was adjusted to obtain maximal intensity and avoid the saturation of the ICCD camera. The plasma light was limited by two diaphragms, 3 mm in diameter, and focused by a concave mirror, 150 mm focal length, on to the entrance slit of the spectrometer. This ensures the observation of a homogeneous column along the plasma with a variation in the electron density and temperature less than 5 per cent (Peláez et al. 2005).

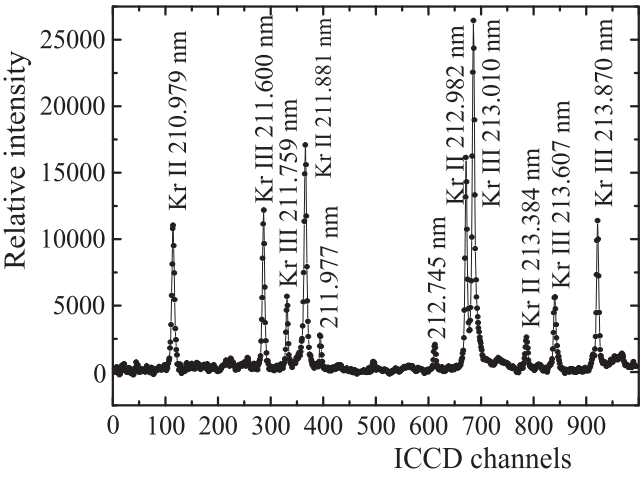

Figure 1. Recorded spectrum of ionized krypton.

The possible self-absorption effect was checked by means of a mirror placed behind the discharge tube. The pressure of the krypton was adjusted to obtain maximal intensity with minimal self-absorption, which allows us to reconstruct the line profile very precisely. All the lines whose self-absorption was higher than 20 per cent were dismissed. For each instant, 10 different runs were recorded in order to increase the signal-to-noise ratio. Three of these profiles were recorded with the self-absorption control mirror and seven without it. The consecutive spectra registered for the same plasma conditions differ in less than 5 per cent. One of the recorded spectra of ionized krypton is shown in Fig. 1. It can be seen from this figure that the recorded spectral line profiles were clear and well defined. This allows us to obtain high-quality experimental parameters.

2.2 Plasma diagnostics

Special care was taken with the plasma diagnostic. Spectroscopic and interferometric end-on measurements have been made simultaneously throughout the plasma life. The measurements have been taken 2 mm off the lamp axis from symmetrical positions referred to it. For the electron density determination, a two-wavelength interferometric technique was applied by making two laser beams of 543.5 and 632.8 nm to pass through the discharge tube in the axial direction. The discharge tube was placed in one of the arms of a Michelson interferometer with a Twyman–Green configuration. This two-wavelength interferometric method allows us to account for the contribution of the heavy particles to the change of the refractivity index (Aparicio et al. 1998). The high-axial homogeneity and the very good cylindrical symmetry of the electron density and the temperature in this lamp (Val et al. 1998) allow this. The electron density, in the range of (1.5–3.4) $\times$ 10^{22} m^{-3}, was obtained with estimated errors between 5 and 10 per cent.

A good determination of the electron temperature is a very important aspect in the measurement of the transition probabilities. The Kr II excitation temperature was obtained from the Boltzmann-plot of some measured Kr II lines for which the transition probabilities were taken from the bibliography. We will refer to

Table 1. Selected wavelengths and transition probabilities from Kramida et al. (2015) – KRA – and Mar et al. (2006) – MAR – for the temperature determination.

Wavelength (nm)	E_k (eV)	g_k	$A_{\rm ref}$ ($10^8 s^{-1}$)	Ref.	$A_{\rm TW}$ ($10^8 s^{-1}$)
459.280	21.321	6	0.203	MAR	0.203
460.402	20.070	2	0.272	MAR	0.282
461.529	17.375	4	0.487	KRA	0.471
461.917	17.372	6	0.655	KRA	0.648
482.519	17.571	4	0.240	KRA	0.229
483.208	16.835	2	0.745	KRA	0.832
484.661	17.246	2	0.769	MAR	0.759

these lines as the reference lines. The transition probability values for these lines, $A_{\rm ref}$, were taken from Kramida et al. (2015) and from Mar et al. (2006). The transition probabilities taken from Kramida et al. (2015) are classified like D by National Institute of Standards and Technology (NIST). The criterion used to select the reference lines was to use data from Kramida et al. (2015) in all cases except for those lines not measured and for which Mar et al. (2006) provide data. It is important to notice that the values from Kramida et al. (2015) belong to the doctoral thesis of Helbig (1978). These values were measured in a wall-stabilized arc and the population densities were calculated under the assumption of local thermodynamic equilibrium (LTE). Regarding the values from Mar et al. (2006), they were also derived by using the absolute scale proposed by Helbig (1978) and measured in an emission spectroscopy experiment by using a similar experimental set-up as the one described in this work, but with a different radiation detector. In Table 1, all the reference lines with their corresponding transition probabilities $A_{\rm ref}$ (Mar et al. 2006; Kramida et al. 2015) and energy values E_k (Kramida et al. 2015) are given. The third column contains the transition probability values measured in this work for the reference lines, $A_{\rm TW}$. The relative uncertainty of these $A_{\rm TW}$ values introduced by our measuring method is around 10 per cent.

Fig. 2 shows the Boltzmann plots for each measurement instant throughout the life of the plasma, as well as the excitation temperature for the different instants. According to van der Mullen (1990), the excitation temperature takes similar values to the kinetic temperature in collision-dominated plasmas, like the plasma produced in this experiment. The linearity of the Boltzmann plots, with R^2 values of around 0.99, supports the assumption that our plasma is well described by a pLTE model, at least within the interval of the upper energy levels considered (17–21.5 eV). An additional check shows that pLTE is satisfied in this experiment for the atomic states whose principal quantum number is larger than 3 and for electron densities larger than 10^{22} m^{-3} (Griem 1963, 1997). This supports the existence of pLTE for all the upper energy levels considered in this work. The uncertainty in the temperature was calculated from the standard deviation of the slope in a non-weighted linear fit of the Boltzmann plot and it turned to be 5 per cent. If we include the uncertainties of the reference data by performing a weighted linear fit, this uncertainty raises up to 25 per cent.

3 TRANSITION PROBABILITY DATA DETERMINATION

The transition probability values were obtained by measuring the relative intensities of the spectral lines under study and using the transition probability data taken from the bibliography (Mar et al. 2006; Kramida et al. 2015) for the seven lines used as a reference.

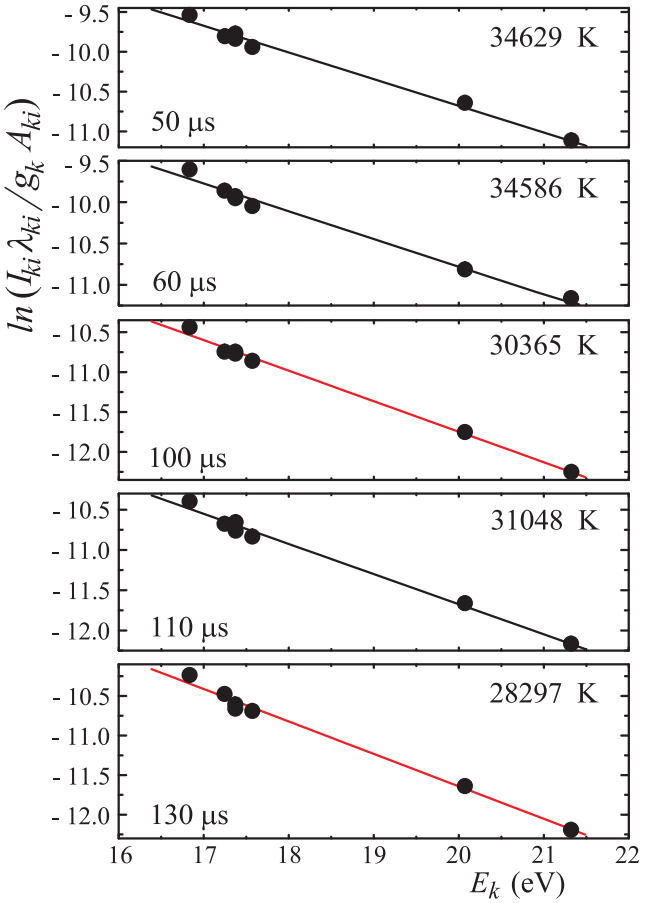

Figure 2. Boltzmann plots for different plasma instants.

Before carrying on with any calculations, the recorded spectra were corrected by the spectral response of the optical and the spectroscopic system. For that purpose, we used an calibrated incandescent lamp which emits like a blackbody at 3041 K for the visible region and a calibrated deuterium lamp for the UV. The uncertainty of the transmittance curve was estimated to be lower than 4 per cent. The corrected spectra were fitted to sums of Lorentzian functions, which represent the spectral line profiles, and a linear function, which represents the emission from the continuum (Djurović et al. 2006). The areas under the profiles were considered as the relative line intensities that were used for the determination of the transition probabilities. From the ratio between the intensity of two spectral lines of the same species and stage of ionization (the line under study and a reference line) and considering the equilibrium assumption, it is possible to obtain the equation 34 in Konjević (1999). Rearranging this equation, we can isolate the unknown transition probability value and express it as a function of known quantities:

$$A_{\rm ki} = A_{\rm ref}\frac{I_{\rm ki}}{I_{\rm ref}}\frac{\lambda_{\rm ki}}{\lambda_{\rm ref}}\frac{g_{\rm ref}}{g_{\rm k}}\exp^{\frac{E_{\rm ki}-E_{\rm ref}}{\rm kT}}, \quad (1)$$

where g are the statistical weights and E the upper energy level of the considered transitions. This procedure was repeated for the five instants of the plasma life for which spectroscopic measurements were performed and using the intensities of the seven spectral lines used as reference (Table 1) and whose transition probabilities, $A_{\rm ref}$, were taken from the bibliography (Mar et al. 2006; Kramida et al. 2015). As a whole, we obtained 35 values of $A_{\rm ki}$ for each of the spectral lines. The final $A_{\rm ki}$ result for each line was determined by

means of a weighted arithmetic mean. We calculated the weights from the uncertainty associated with our measurement of the area for every spectral line (Belmonte et al. 2014). This relative uncertainty was calculated by taking into account different aspects, such us the accuracy of the fitting, the self-absorption of the spectral line, the ratio between the background intensity and the maximum height of the line and the overlapping with the adjacent spectral lines. All these factors were added in quadrature to get the final value of the relative uncertainty.

4 EXPERIMENTAL RESULTS AND DISCUSSION

The experimentally obtained transition probability data for the Kr II spectral lines are given in Table 2. The table is arranged in order of increasing wavelength. The first column contains the wavelengths of the observed spectral lines, followed by the configuration, term and J value of the upper and lower energy levels of each transition. The notation for most of them has been taken from Kramida et al. (2015). The last column includes our transition probability results, A_{TW}, with their relative uncertainties in per cent shown in parentheses. As explained before, these relative uncertainties have been carefully calculated by following the method described in Belmonte et al. (2014). We would like to emphasize that the relative uncertainties included in Table 2 are the ones introduced by our experimental procedure and they do not take into account the uncertainty of the transition probabilities used as reference. The absolute uncertainty could be calculated by adding in quadrature our relative uncertainty and the one estimated by NIST for the reference A_{ki} values.

Several of the transitions in Table 2 present some characteristics and peculiarities which are worth mentioning.

(1) The line 210.979 nm is notated as $4s^24p^4(^3P)4d^4D_{3/2} - 4s^24p^4(^3P_2)4f^2[2]^o_{3/2}$ in our Table 2 and it has a relative intensity of 5 in Kramida et al. (2015). In this data base, there is an additional and very close line (210.988 nm) with the transition $4s^24p^4(^3P)5s^2P_{1/2} - 4s^24p^4(^3P_2)4f^2[2]^o_{3/2}$ and a relative intensity of 3. However, there is only one line at this wavelength, 210.981 nm, in Striganov & Sventitskii (1968) with the transition $4d^4D_{3/2} - 5f^2F^o_{3/2}$. From our recorded spectrum and fitting procedure, and keeping in mind that the spectral resolution of our spectrometer is around 3 pm per channel (Peláez et al. 2012), we can conclude that only one spectral line appears in our experiment (see Fig. 1).

(2) The terms and J values for the lower energy levels of 12 spectral lines are missing. Although the LS-coupling scheme has been used to describe the $4s^24p^4(^3P)4d$ levels, the coupling is not a pure LS one due to the mixing obtained with most of the levels of this configuration (El Sherbini & Farrag 1976). The maximum percentage of the components in the composition of these levels is 35 per cent. For this reason, the levels are not dominated by a particular component and they are only described by the total angular momentum.

(3) The configuration, term and J value for the upper and lower energy levels of seven of the spectral lines given in Table 2 are missing in Kramida et al. (2015). In this case, we used the notation from Striganov & Sventitskii (1968), even though it is also incomplete.

Due to the lack of experimental data for transition probabilities in the UV region (208–360 nm), there is only a small number of results from other authors to compare with our results. Some relative transition probability values are given in Fonseca & Campos (1982) and some absolute ones in Podbiralina et al. (1973) and Dzierżega et al. (2001). The comparison among the absolute values is given in Table 3. The absolute results from Dzierżega et al. (2001) are in a relative good agreement with ours and they will be analysed in detail later. The comparison with Podbiralina et al. (1973) shows considerable discrepancies with both Dzierżega et al. (2001) and A_{TW}.

In Fig. 3, we compare our transition probability results, A_{TW}, with the experimental ones from Dzierżega et al. (2001), A_{DZ}. The work of Dzierżega et al. (2001) provides absolute transition probabilities for transitions from 5p and 5p' levels between 200 and 2400 nm determined by normalizing the experimentally measured branching ratios with a weighted mean of published upper level lifetime data. As can be seen from Fig. 3, the A_{DZ} values show a very good agreement with ours. The linear regression fit has a y-intercept of 0.036 ± 0.034 and a slope of 1.27 ± 0.085. It is possible to observe how the A_{ki} values in Fig. 3 are, in general, randomly distributed along the linear regression fit line, giving a R^2 value of 0.98. The fact that the y-intercept is almost zero seems natural since the transition probability values of the lines under study range between almost zero to one. This y-intercept reveals, among other things, that the spectral lines have been properly identified. The fact that the R^2 value is so close to one reflects the fact that our values (A_{TW}) and those from Dzierżega et al. (2001) (A_{DZ}) are in a relative good agreement. We can observe how the values from Dzierżega et al. (2001) and from our work could be taken as equivalent if we consider the 20 per cent of uncertainty inherent to the quantitative spectroscopy methods.

Two different aspects should be born in mind when trying to evaluate this discrepancy between our values and those from Dzierżega et al. (2001): the quality of the measurements made and the scale used to transform these measurements into absolute transition probability values. These two aspects can be evaluated both for A_{DZ} and A_{TW}. On the one hand, regarding A_{TW}, the relative intensities of the spectral lines were carefully measured to avoid any kind of systematic error. In this case, the values from the thesis of Helbig (1978) constitute the absolute scale selected by us to transform our relative measurements to absolute ones, since all the data measured in our laboratory (de Castro et al. 2001; Rodríguez et al. 2001; Mar et al. 2006) come from this scale. The A_{ki} values from the thesis of Helbig (1978) have been traditionally considered to be some of the most accurate data available for Kr II (Ward et al. 1985), as proves the fact that they have been selected for several compilations and handbooks of basic atomic spectroscopic data (Fuhr & Wiese 1996, 1998; Sansonetti & Martin 2005). On the other hand, the branching ratios measured by Dzierżega et al. (2001) were normalized to absolute transition probabilities by using a weighted mean value calculated from very carefully chosen values of upper-level lifetimes. This set of lifetimes defines the Dzierżega et al. (2001) scale.

Both types of experiments, Dzierżega et al. (2001) and this work, have strengths and weaknesses and it is very difficult to establish which the absolute scale is. However, Fig. 3 reveals that both absolute scales are not so different and it makes it possible to relate them in a precise and simple way. Since the y-intercept is almost null within its error bar and the R^2 is close to 1, both sets of values A_{DZ} and A_{TW} are simply related by a factor, which implies that rescaling our data to those from Dzierżega et al. (2001) can be done easily just by using the slope of the fitting in Fig. 3. The data from Helbig (1978) and Mar et al. (2006) and therefore, ours in this work, present a good agreement and can be adjusted to another absolute scale by using an appropriate scaling factor. The Boltzmann plots with all our measured A_{ki} data for every instant have been used as a way of checking the general behaviour of our results. Fig. 4 shows

Table 2. Measured transition probability data for the Kr II spectral transitions.

λ (nm)	E_{upper} (eV)	E_{lower} (eV)	Upper level Conf.	Term	J	Lower level Conf.	Term	J	A_{TW} (10^8 s^{-1})
208.673	20.844	14.904	$4s^24p^4(^3P_2)4f$	$^2[4]^o$	7/2	$4s^24p^4(^3P)4d$	^4D	7/2	0.24(11)
208.815	20.840	14.904	$4s^24p^4(^3P_2)4f$	$^2[4]^o$	9/2	$4s^24p^4(^3P)4d$	^4D	7/2	0.700(11)
209.337	20.852	14.931	$4s^24p^4(^3P_2)4f$	$^2[3]^o$	5/2	$4s^24p^4(^3P)4d$	^4D	5/2	0.36(11)
209.623	20.844	14.931	$4s^24p^4(^3P_2)4f$	$^2[4]^o$	7/2	$4s^24p^4(^3P)4d$	^4D	5/2	0.600(11)
210.979	20.877	15.002	$4s^24p^4(^3P_2)4f$	$^2[2]^o$	3/2	$4s^24p^4(^3P)4d$	^4D	3/2	0.52(11)
211.881	20.852	15.002	$4s^24p^4(^3P_2)4f$	$^2[3]^o$	5/2	$4s^24p^4(^3P)4d$	^4D	3/2	0.51(11)
221.172	21.465	15.861	$4s^24p^4(^3P_1)4f$	$^2[3]^o$	7/2	$4s^24p^4(^3P)4d$	^4F	7/2	0.022(15)
221.296	21.421	15.820	$4s^24p^4(^3P_1)4f$	$^2[2]^o$	5/2	$4s^24p^4(^1D)5s$	^2D	3/2	0.033(14)
222.793	21.425	15.861	$4s^24p^4(^3P_1)4f$	$^2[4]^o$	9/2	$4s^24p^4(^3P)4d$	^4F	7/2	0.24(11)
228.779	21.27	15.85	$4s^24p^4(^1D)5d$	6^o	7/2	5s’	^2D	5/2	0.49(11)
230.174	21.465	16.080	$4s^24p^4(^3P_1)4f$	$^2[3]^o$	7/2	$4s^24p^4(^3P)4d$	^4F	5/2	0.069(11)
231.202	18.875	13.514	$4s^24p^4(^1D)5p$	$^2P^o$	1/2	$4s4p^6$	^2S	1/2	0.084(11)
231.424	21.414	16.058	$4s^24p^4(^3P_1)4f$	$^2[2]^o$	3/2	$4s^24p^44d$		1/2	0.22(11)
231.553	21.534	16.182	$4s^24p^4(^3P_0)4f$	$^2[3]^o$	5/2	$4s^24p^4(^3P)4d$	^4F	3/2	0.34(11)
234.438	21.468	16.182	$4s^24p^4(^3P_1)4f$	$^2[3]^o$	5/2	$4s^24p^4(^3P)4d$	^4F	3/2	0.32(11)
235.287	20.890	15.622	$4s^24p^4(^3P_2)4f$	$^2[5]^o$	9/2	$4s^24p^4(^3P)4d$	^4F	9/2	0.013(14)
236.275	21.534	16.289	$4s^24p^4(^3P_0)4f$	$^2[3]^o$	5/2	$4s^24p^4(^3P)4d$	^2P	3/2	0.11(11)
237.369	20.844	15.622	$4s^24p^4(^3P_2)4f$	$^2[4]^o$	7/2	$4s^24p^4(^3P)4d$	^4F	9/2	0.042(11)
237.553	20.840	15.622	$4s^24p^4(^3P_2)4f$	$^2[4]^o$	9/2	$4s^24p^4(^3P)4d$	^4F	9/2	0.17(11)
239.279	21.468	16.289	$4s^24p^4(^3P_1)4f$	$^2[3]^o$	5/2	$4s^24p^4(^3P)4d$	^2P	3/2	0.12(13)
240.852	21.751	16.604	$4s^24p^4(^3P)6d$	^4D	5/2	$4s^24p^4(^3P)5p$	$^4P^o$	5/2	0.12(12)
240.907	21.465	16.320	$4s^24p^4(^3P_1)4f$	$^2[3]^o$	7/2	$4s^24p^4(^3P)4d$	^2F	7/2	0.054(11)
241.381	21.739	16.604	$4s^24p^4(^3P)6d$	^4D	7/2	$4s^24p^4(^3P)5p$	$^4P^o$	5/2	0.14(11)
241.840	21.414	16.289	$4s^24p^4(^3P_1)4f$	$^2[2]^o$	3/2	$4s^24p^4(^3P)4d$	^2P	3/2	0.11(13)
245.607	21.533	16.486	$4s^24p^4(^3P_0)4f$	$^2[3]^o$	7/2	$4s^24p^4(^3P)4d$	^4P	5/2	0.29(11)
246.477	20.890	15.861	$4s^24p^4(^3P_2)4f$	$^2[5]^o$	9/2	$4s^24p^4(^3P)4d$	^4F	7/2	0.700(13)
247.885	20.861	15.861	$4s^24p^4(^3P_2)4f$	$^2[3]^o$	7/2	$4s^24p^4(^3P)4d$	^4F	7/2	0.043(11)
250.387	21.27	16.32		6^o	7/2	4d	^2F	7/2	0.29(10)
255.591	20.907	16.058	$4s^24p^4(^3P_2)4f$	$^2[1]^o$	1/2	$4s^24p^44d$		1/2	0.24(14)
255.636	21.533	16.684	$4s^24p^4(^3P_0)4f$	$^2[3]^o$	7/2	$4s^24p^4(^3P)4d$	^2F	5/2	0.085(11)
255.910	21.534	16.691	$4s^24p^4(^3P_0)4f$	$^2[3]^o$	5/2	$4s^24p^44d$		3/2	0.13(11)
259.125	22.030	17.246	$4s^24p^4(^1D)5d$	^2P	3/2	$4s^24p^4(^3P)5p$	$^2P^o$	1/2	0.047(13)
259.248	21.465	16.684	$4s^24p^4(^3P_1)4f$	$^2[3]^o$	7/2	$4s^24p^4(^3P)4d$	^2F	5/2	0.74(11)
259.440	21.468	16.691	$4s^24p^4(^3P_1)4f$	$^2[3]^o$	5/2	$4s^24p^44d$		3/2	0.045(12)
259.536	20.86	16.09	5p”	$^2P^o$	1/2	4d	^4F	3/2	0.300(11)
259.773	20.852	16.080	$4s^24p^4(^3P_2)4f$	$^2[3]^o$	5/2	$4s^24p^4(^3P)4d$	^4F	5/2	0.073(11)
260.211	20.844	16.080	$4s^24p^4(^3P_2)4f$	$^2[4]^o$	7/2	$4s^24p^4(^3P)4d$	^4F	5/2	0.048(11)
261.671	21.421	16.684	$4s^24p^4(^3P_1)4f$	$^2[2]^o$	5/2	$4s^24p^4(^3P)4d$	^2F	5/2	0.12(11)
262.775	20.946	16.229	$4s^24p^4(^1S)5p$	$^2P^o$	3/2	$4s^24p^4(^3P)4d$	^4P	1/2	0.075(12)
264.306	20.918	16.229	$4s^24p^4(^3P_2)4f$	$^2[1]^o$	3/2	$4s^24p^4(^3P)4d$	^4P	1/2	0.31(11)
264.927	20.907	16.229	$4s^24p^4(^3P_2)4f$	$^2[1]^o$	1/2	$4s^24p^4(^3P)4d$	^4P	1/2	0.42(13)
266.097	21.528	16.870	$4s^24p^4(^3P)7s$	^4P	3/2	$4s^24p^4(^3P)5p$	$^4D^o$	5/2	0.16(12)
266.400	21.487	16.835	$4s^24p^4(^3P)7s$	^4P	5/2	$4s^24p^4(^3P)5p$	$^4D^o$	7/2	0.11(11)
266.661	20.877	16.229	$4s^24p^4(^3P_2)4f$	$^2[2]^o$	3/2	$4s^24p^4(^3P)4d$	^4P	1/2	0.063(11)
268.355	20.907	16.289	$4s^24p^4(^3P_2)4f$	$^2[1]^o$	1/2	$4s^24p^4(^3P)4d$	^2P	3/2	0.300(12)
269.570	20.886	16.289	$4s^24p^4(^3P_2)4f$	$^2[2]^o$	5/2	$4s^24p^4(^3P)4d$	^2P	3/2	0.18(13)
271.240	20.890	16.320	$4s^24p^4(^3P_2)4f$	$^2[5]^o$	9/2	$4s^24p^4(^3P)4d$	^2F	7/2	0.37(10)
271.449	20.886	16.320	$4s^24p^4(^3P_2)4f$	$^2[2]^o$	5/2	$4s^24p^4(^3P)4d$	^2F	7/2	0.028(13)
271.616	20.852	16.288	$4s^24p^4(^3P_2)4f$	$^2[3]^o$	5/2	$4s^24p^4(^3P)4d$	^2P	3/2	0.046(11)
272.946	20.861	16.320	$4s^24p^4(^3P_2)4f$	$^2[3]^o$	7/2	$4s^24p^4(^3P)4d$	^2F	7/2	0.082(11)
273.233	21.534	16.998	$4s^24p^4(^3P_0)4f$	$^2[3]^o$	5/2	$4s^24p^44d$		5/2	0.020(14)
273.326	21.533	16.998	$4s^24p^4(^3P_0)4f$	$^2[3]^o$	7/2	$4s^24p^44d$		5/2	0.21(11)
274.256	20.840	16.320	$4s^24p^4(^3P_2)4f$	$^2[4]^o$	9/2	$4s^24p^4(^3P)4d$	^2F	7/2	0.098(11)
275.902	22.064	17.571	$4s^24p^4(^3P)7s$	^2P	3/2	$4s^24p^4(^3P)5p$	$^4S^o$	3/2	0.038(16)
277.260	21.468	16.998	$4s^24p^4(^3P_1)4f$	$^2[3]^o$	5/2	$4s^24p^44d$		5/2	0.025(11)
279.581	21.431	16.998	$4s^24p^4(^3P_1)4f$	$^2[4]^o$	7/2	$4s^24p^44d$		5/2	0.28(10)
280.320	20.907	16.486	$4s^24p^4(^3P^2)4f$	$^2[1]^o$	1/2	$4s^24p^44d$		3/2	0.18(11)

the Boltzmann plot for the instant 60 μs after the beginning of the discharge. The deviation from the line obtained by a least-square fitting procedure is within ± 3 per cent. It is similar for any other instant of the plasma life for which measurements were taken. These results confirm the validity and self-consistency of our experimental transition probability data.

From the slope of the Boltzmann plot shown in Fig. 4, we obtain an electron temperature of 34 585 K. This temperature is in

Table 2 – *continued*

λ (nm)	E_{upper} (eV)	E_{lower} (eV)	Upper level Conf.	Term	J	Lower level Conf.	Term	J	A_{TW} (10^8 s^{-1})
280.360	20.91	16.48	5f	$^2D^o$	3/2		1	5/2	0.022(24)
281.646	20.886	16.486	$4s^24p^4(^3P_2)4f$	$^2[2]^o$	5/2	$4s^24p^44d$		3/2	0.300(11)
281.687	20.886	16.486	$4s^24p^4(^3P_2)4f$	$^2[2]^o$	5/2	$4s^24p^4(^3P)4d$	^4P	5/2	0.14(12)
283.300	20.861	16.486	$4s^24p^4(^3P_2)4f$	$^2[3]^o$	7/2	$4s^24p^4(^3P)4d$	^4P	5/2	0.29(10)
283.879	20.852	16.486	$4s^24p^4(^3P_2)4f$	$^2[3]^o$	5/2	$4s^24p^44d$		3/2	0.057(11)
284.446	20.844	16.486	$4s^24p^4(^3P_2)4f$	$^2[4]^o$	7/2	$4s^24p^4(^3P)4d$	^4P	5/2	0.028(11)
284.738	18.623	14.270	$4s^24p^4(^1D)5p$	$^2P^o$	3/2	$4s^24p^4(^3P)5s$	^4P	3/2	0.041(11)
295.835	22.73	18.54		13^o	5/2	4d’	^2D	5/2	0.088(12)
296.725	20.861	16.684	$4s^24p^4(^3P_2)4f$	$^2[3]^o$	7/2	$4s^24p^4(^3P)4d$	^2F	5/2	0.14(11)
297.404	20.852	16.684	$4s^24p^4(^3P_2)4f$	$^2[3]^o$	5/2	$4s^24p^4(^3P)4d$	^2F	5/2	0.035(11)
297.887	20.852	16.691	$4s^24p^4(^3P_2)4f$	$^2[3]^o$	5/2	$4s^24p^44d$		3/2	0.049(11)
306.084	20.70	16.65		11^o	5/2		^2D	3/2	0.073(11)
315.094	18.623	14.689	$4s^24p^4(^1D)5p$	$^2P^o$	3/2	$4s^24p^4(^3P)5s$	^2P	3/2	0.12(11)
320.040	18.875	15.002	$4s^24p^4(^1D)5p$	$^2P^o$	1/2	$4s^24p^4(^3P)5s$	^2P	1/2	0.13(11)
320.828	17.378	13.514	$4s^24p^4(^3P)5p$	$^4D^o$	1/2	$4s4p^6$	^2S	1/2	0.12(12)
322.657	22.66	18.82		10^o	3/2		^2P	3/2	0.058(17)
328.209	18.875	15.099	$4s^24p^4(^1D)5p$	$^2P^o$	1/2	$4s^24p^4(^3P)4d$	^4D	1/2	0.040(11)
337.903	21.041	17.372	$4s^24p^4(^3P)5d$	^2D	5/2	$4s^24p^4(^3P)5p$	$^2D^o$	5/2	0.040(12)
338.111	21.041	17.375	$4s^24p^4(^3P)5d$	^2D	5/2	$4s^24p^4(^3P)5p$	$^2P^o$	3/2	0.073(11)
338.523	20.818	17.157	$4s^24p^4(^3P)5d$	^2P	3/2	$4s^24p^4(^3P)5p$	$^4D^o$	3/2	0.055(11)
342.373	18.623	15.002	$4s^24p^4(^1D)5p$	$^2P^o$	3/2	$4s^24p^4(^3P)5s$	^2P	1/2	0.027(11)
342.771	17.605	13.989	$4s^24p^4(^3P)5p$	$^2D^o$	3/2	$4s^24p^4(^3P)5s$	^4P	5/2	0.037(11)
343.098	20.769	17.157	$4s^24p^4(^3P)5d$	^4P	5/2	$4s^24p^4(^3P)5p$	$^4D^o$	3/2	0.042(12)
346.541	21.148	17.571	$4s^24p^4(^3P)5d$	^2D	3/2	$4s^24p^4(^3P)5p$	$^4S^o$	3/2	0.030(13)
347.005	20.818	17.246	$4s^24p^4(^3P)5d$	^2P	3/2	$4s^24p^4(^3P)5p$	$^2P^o$	1/2	0.29(11)
350.325	22.033	18.495	$4s^24p^4(^1D)5d$	^2F	5/2	$4s^24p^4(^1D)5p$	$^2F^o$	5/2	0.29(11)
353.535	20.155	16.649	$4s^24p^4(^3P)5d$	^4D	1/2	$4s^24p^4(^3P)5p$	$^4P^o$	3/2	0.49(10)
354.414	21.148	17.651	$4s^24p^4(^3P)5d$	^2D	3/2	$4s^24p^4(^3P)5p$	$^2S^o$	1/2	0.49(14)
354.454	22.058	18.561	$4s^24p^4(^1D)5d$	^2F	7/2	$4s^24p^4(^1D)5p$	$^2F^o$	7/2	0.36(12)
355.349	20.093	16.604	$4s^24p^4(^3P)5d$	^4D	3/2	$4s^24p^4(^3P)5p$	$^4P^o$	5/2	0.14(11)
355.554	22.109	18.623	$4s^24p^4(^1D)5d$	^2D	5/2	$4s^24p^4(^1D)5p$	$^2P^o$	3/2	0.16(12)
357.268	21.041	17.571	$4s^24p^4(^3P)5d$	^2D	5/2	$4s^24p^4(^3P)5p$	$^4S^o$	3/2	0.061(11)
358.625	20.061	16.604	$4s^24p^4(^3P)6s$	^2P	3/2	$4s^24p^4(^3P)5p$	$^4P^o$	5/2	0.042(11)
358.965	20.699	17.246	$4s^24p^4(^3P)5d$	^2P	1/2	$4s^24p^4(^3P)5p$	$^2P^o$	1/2	0.83(10)
359.686	20.818	17.372	$4s^24p^4(^3P)5d$	^2P	3/2	$4s^24p^4(^3P)5p$	$^2D^o$	5/2	0.028(15)
359.921	20.818	17.375	$4s^24p^4(^3P)5d$	^2P	3/2	$4s^24p^4(^3P)5p$	$^2P^o$	3/2	0.26(12)

Table 3. Comparison of the transition probabilities from this work (TW) with the absolute results from Dzierżega et al. (2001) – DZ – and Podbiralina et al. (1973) – PSS.

Wavelength (nm)	Absolute A_{ki} (10^8 s^{-1}) TW	DZ	PSS
231.202	0.084	0.054	
342.771	0.037	0.049	
284.738	0.041	0.072	0.130
315.094	0.12	0.210	0.045
320.040	0.13	0.227	
342.373	0.027	0.038	
328.209	0.040	0.060	

a very good agreement with the one obtained from the measurements of the excitation temperature. This is the confirmation that our experimental procedure has been performed properly.

5 CONCLUSIONS

As a final conclusion, this work reports transition probability values for a set of 93 Kr II lines in the spectral region ranging from 208 to 360 nm, extending considerably the transition probability data base

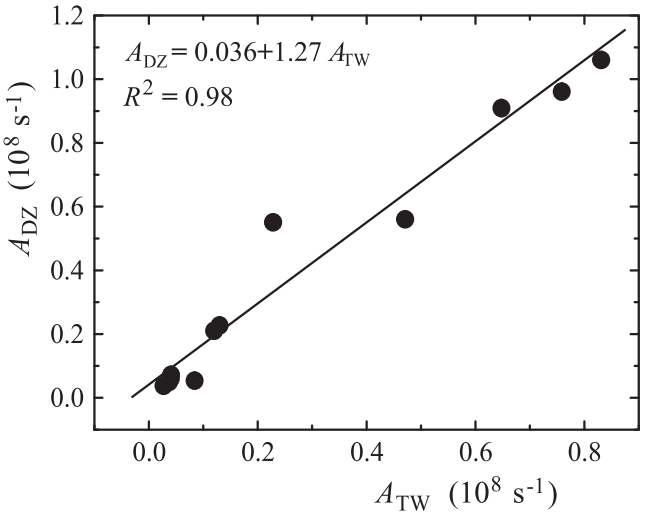

Figure 3. Comparison between the absolute transition probabilities from Dzierżega et al. (2001), A_{DZ}, and those from this work, A_{TW}.

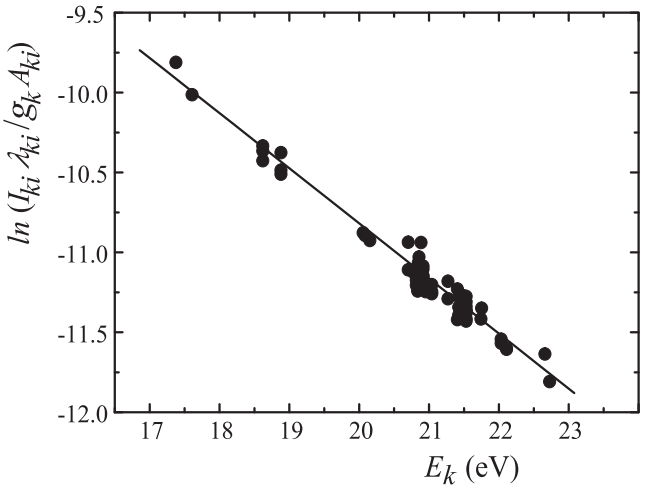

Figure 4. One of the Boltzmann plots obtained from all the new transition probability data presented in this work.

in the UV. For 86 of them there are not previous data, at least up to the authors' knowledge. The relative uncertainties of the A_{ki} values introduced by our method of measuring have been carefully calculated by taking into account different sources of error and they are lower than 15 per cent for almost all of them. Furthermore, this work analyses the differences found between data from Dzierżega et al. (2001), which constitutes one of the most comprehensive works done recently in A_{ki} values for Kr II, and the new values presented in this work. Since a careful revision of lifetime experiments was made in Dzierżega et al. (2001), the comparison with our data provides a useful mathematical expression to relate the A_{ki} values normalized with a scale based on lifetime measurements with those obtained from a scale based on plasma emission spectroscopy measurements. However, a very precise measurement of the value of at least one absolute transition probability would provide a way to establish the most appropriate absolute scale.

ACKNOWLEDGEMENTS

We thank S. González for all his work and help with the experimental set-up. MTB acknowledges financial support from the University of Valladolid through the FPI PhD grant. LG and SD thank the Ministry of Education, Science and Technological development of Republic Serbia for support under Project 171014. RJP acknowledges the grant JCI-2012-13034 from the Juan de la Cierva Programme.

REFERENCES

Aparicio J. A., Gigosos M. A., González V. R., Pérez C., de la Rosa M. I., Mar S., 1998, J. Phys. B: At. Mol. Opt. Phys., 31, 1029
Belmonte M. T., Djurović S., Peláez R. J., Aparicio J. A., Mar S., 2014, MNRAS, 445, 3345
Bertuccelli G., Di Rocco H. O., 1991, Spectrosc. Lett., 24, 1039
Bidelman W. P., 1962, ApJ, 67, 111
Brandt T., Helbig V., Nick K.-P., 1982, J. Phys. B: At. Mol. Phys., 15, 2139
Cardelli J. A., Meyer D. M., 1997, ApJ, 477, L57
Cardelli J. A., Savage B. D., Ebbets D. C., 1991, ApJ, 383, L23
Cayless M. A., Marsden A. M., 1983, Lamps and Lighting, 3rd edn. Edward Amold, London
Ćirišan M., Peláez R. J., Djurović S., Aparicio J. A., Mar S., 2011, Phys. Rev. A, 83, 012513
Das M. B., 1997, J. Quant. Spectrosc. Radiat. Transfer, 57, 237
Das M. B., Bhattacharya R., 1992, Z. Phys., 22, 699
de Castro A., Aparicio J. A., del Val J. A., González V. R., Mar S., 2001, J. Phys. B: At. Mol. Opt. Phys., 34, 3275
del Val J. A., Mar S., Gigosos M. A., de la Rosa M. I., Pérez C., González V. R., 1998, Japan. J. Appl. Phys., 37, 4177
Dinerstein H. L., 2001, ApJ, 550, L223
Djeniže S., Milosavljević V., Dimitrijević M. S., 2003, Eur. Phys. J. D, 27, 209
Djurović S., Peláez R. J., Ćirišan M., Aparicio J. A., Mar S., 2006, J. Phys. B: At. Mol. Opt. Phys., 39, 2901
Dzierżega K., Griesmann U., Nave G., Bratasz L., 2001, Phys. Scr., 63, 209
El Sherbini T. M., Farrag A. A., 1976, J. Phys. B: At. Mol. Opt. Phys., 9, 2797
Fonseca V., Campos J., 1982, J. Phys. B: At. Mol. Phys., 15, 2349
Fuhr J. R., Wiese W. L., 1996, in Lide D. R., Frederikse H. P. R., eds, CRC Handbook of Chemistry and Physics, 77th edn., CRC Press. Inc., Boca Raton, p. 128
Fuhr J. R., Wiese W. L., 1998, in Lide D. R., ed., CRC Handbook of Chemistry and Physics, 78th edn. CRC Press. Inc., Boca Raton, p. 154
Gigosos M. A., Mar S., Pérez C., de la Rosa I., 1994, Phys. Rev. E, 49, 1575
Griem H. R., 1963, Phys. Rev., 131, 1170
Griem H. R., 1964, Plasma Spectroscopy. McGraw-Hill Book Company, New York
Griem H. R., 1997, Principles of Plasma Spectroscopy. Cambridge Univ. Press, Cambridge
Helbig V., 1978, PhD thesis, Kiel Univ.
Jullien S., Lemaire J., Fenistein S., Heninger M., Mauclaire G., Marx R., 1993, Chem. Phys. Lett., 212, 340
Konjević N., 1999, Phys. Rep., 316, 339
Kramida A., Ralchenko Yu., Reader J., NIST ASD Team, 2015, NIST Atomic Spectra Database (version 5.2), (Available at http://physics.nist.gov/asd)
Lauer S., Liebel H., Vollweiler F., Schmoranzer H., Lagutin B. M., Demekhin Ph. V., Petrov I. D., Sukhorukov V. L., 1999, J. Phys. B: At. Mol. Phys., 32, 2015
Loch S. D. et al., 2002, Phys. Rev. A, 66, 052708
Mar S., del Val J. A., Rodríguez F., Peláez R. J., González V. R., Gonzalo A. B., de Castro A., Aparicio J. A., 2006, J. Phys. B: At. Mol. Phys., 39, 3709
Marantz H., Rudko R. I., Tang C. L., 1969, IEEE J. Quantum Electron., 5, 38
Mazouffre S., Pawelec E., 2009, J. Phys. D: Appl. Phys., 42, 015203
Miller M. H., Roig R. A., Bengtson R. D., 1972, J. Opt. Soc. Am., 62, 1027
Morton D. C., 2000, ApJS, 130, 403
Peláez R. J., Pérez C., González V. R., Rodríguez F., Aparicio J. A., Mar S., 2005, J. Phys. B., 38, 2505
Peláez R. J., Mar S., Aparicio J. A., Belmonte M. T., 2012, Appl. Spectrosc., 66, No. 8
Podbiralina V. P., Smimov Yu. M., Stegnova N. V., 1973, Opt. Spectrosc., 34, 467
Rodríguez F., Aparicio J. A., de Castro A., del Val J. A., González V. R., Mar S., 2001, A&A, 372, 338
Saito M., Ojima N., Itoi S., Haruyama Y., 2015, Phys. Rev. A, 91, 012508
Sansonetti J. E., Martin W. C., 2005, J. Phys. Chem. Ref. Data, 34, 1559
Schade W., Stryla Z. W., Helbig V., Langhans G., 1989, Phys. Scr., 39, 246
Sharpee B., Zhang Y., Williams R., Pellegrini E., Cavagnolo K., Badwin J. A., Phillips M., Lui X. W., 2007, ApJ, 659, 1265
Shimoda K., 1984, Introduction to Laser Physics. Springer Series in Optical Sciences, Springer, Berlin
Striganov A. R., Sventitskii N. S., 1968, Tables of Spectral Lines of Neutral and Ionized Atoms. Plenum, New York
Träbert E., 2012, Phys. Scr., 85, 048101
van der Mullen J. A. M., 1990, Phys. Rep. 191, 109
Ward L., Wännström A., Arnesen A., Hallin R., Vogel O., 1985, Phys. Scr., 31, 149
Werner K., Rauch T., Ringat E., Kruk J. W., 2012, ApJ, 753, L7

This paper has been typeset from a TEX/LATEX file prepared by the author.